ANTIOXIDANTS & REDOX SIGNALING
Volume 8, Numbers 7 & 8, 2006

Forum Original Research Communication

Manganese Superoxide Dismutase Protects from TNF-α–Induced Apoptosis by Increasing the Steady-State Production of H_2O_2

JAYA DASGUPTA,[1,5] SITA SUBBARAM,[1,5] KIP M. CONNOR,[1] ANA M. RODRIGUEZ,[1] OREN TIROSH,[4] JOSEPH S. BECKMAN,[3] DAVID JOURD'HEUIL,[2] and J. ANDRÉS MELENDEZ[1]

ABSTRACT

Manganese superoxide dismutase (SOD2) has been well established to be essential for protection from a variety of apoptotic stimuli. Here we demonstrate that the antiapoptotic effects of SOD2 are attributed to its ability to generate H_2O_2 and that its efficient removal resensitizes cells to tumor necrosis factor (TNF)-α–induced apoptosis. SOD2 overexpression in HT-1080 cells leads to a decrease in the fluorescence of the superoxide-sensitive fluorophore, dihydroethidium, and a concomitant increase in oxidation of the H_2O_2-sensitive dye, dichlorodihydrofluorescein diacetate (DCFDA). The rate of aminotriazole-inhibited catalase activity also was increased when SOD2 is overexpressed and reflects a 1.6-fold increase in the steady-state production of H_2O_2. The increase in H_2O_2 was associated with decreased sensitivity to TNF-α–mediated apoptosis, as measured by monitoring the loss of mitochondrial membrane potential (MMP), caspase activation, poly-ADP ribose polymerase (PARP) cleavage, and accumulation of hypodiploid DNA content. Both the increase in H_2O_2 and resistance to TNF-mediated apoptosis were reversed by coexpression of catalase. The lipid hydroperoxide scavengers, β-hydroxytoluene and trolox, and the iron chelator, desferroxamine, showed partial recovery of TNF-induced apoptosis. These findings indicate that increases in the intracellular steady-state production of H_2O_2 by SOD2 can block the activation of key processes fundamental to the process of programmed cell death. *Antioxid. Redox Signal.* 8, 1295–1305.

INTRODUCTION

All aerobic organisms generate reactive oxygen species (ROS) as by-products of normal cellular metabolism (12). The initial reduction of molecular oxygen (O_2) by leak of electrons from the respiratory chain during oxidative phosphorylation produces the superoxide anion ($O_2^{\cdot -}$). Early work by Boveris and Chance (7) demonstrated that 1–2% of the oxygen consumed by the respiratory chain can be converted to this species in the mitochondria. The primary intracellular antioxidant defenses rely on the enzymatic removal of $O_2^{\cdot -}$ and H_2O_2 before their reaction with other macromolecules. Superoxide dismutase 2 (SOD2) is positioned in the mitochondrial matrix to dismute $O_2^{\cdot -}$ at its site of production,

[1]Center for Immunology and Microbial Disease and [2]Cardiovascular Sciences, Albany Medical College, Albany, New York.
[3]Linus Pauling Institute, Environmental Health Sciences Center, Oregon State University, Corvallis, Oregon.
[4]School of Nutritional Sciences, Institute of Biochemistry, Food Science and Nutrition, Faculty of Agricultural, Food and Environmental Quality Sciences, The Hebrew University of Jerusalem, Rehovot 76100, Israel.
[5]The first two authors contributed equally to this work.
[6]Current address of Dr. Connor: KMC, Department of Ophthalmology, Karp Family Research Building, RB11004g, 1 Blackfan Cir, Boston, MA 02115.

to H_2O_2 and O_2. The electron-neutral H_2O_2 is further detoxified by catalase and glutathione peroxidase into O_2 and H_2O or O_2, respectively. Thus, the cell has evolved very efficient mechanisms to restrict damage by ROS to cellular macromolecules.

H_2O_2 has been implicated as a strong inducer of apoptosis in various cell types (10, 11, 28, 40). Apoptosis or programmed cell death refers to a series of tightly coordinated events designed to eliminate potentially dangerous cells and cells that have reached the end of their life cycle. Apoptosis allows an organism to control tightly cell number and tissue size, as well as to protect itself from cells that interfere with homeostasis. Apoptosis is a tightly regulated process whereby a set of cysteine proteases (caspases) are made active through a complex signaling cascade, resulting in degradation of cellular nuclear DNA (1). In contrast to necrosis, apoptosis destroys only the cell in question, with no effect on surrounding cells (20). Apoptosis can be triggered by both extracellular stimuli and intracellular events that mark cellular dysfunction. The hallmarks of apoptosis include membrane blebbing, cytoskeletal disorganization and loss of mitochondrial integrity, and DNA laddering. The ultimate step in apoptosis is the activation of caspases, which act on a number of downstream cellular proteins, inactivating them by cleaving them after an Asp-Xxx sequence. The pro/inactive forms of these enzymes are activated by cleavage by other upstream caspases or via autoactivation. During tumorigenesis, neoplastic cells are able to restrict apoptosis and circumvent cell death, allowing them to gain a foothold *in vivo* (17). Thus, evasion of apoptosis is a survival mechanism for tumor cells.

Tumor necrosis factor (TNF)-α is a cytokine that is produced by cells under stress and induces signaling via binding to its cell-surface receptor. TNF-α, along with cycloheximide (CHX), has been established as a potent inducer of apoptosis in various cell lines (44). One of the primary mechanism of TNF-α/CHX–induced apoptosis involves activation of the receptor-associated death domains that recruit and activate caspase-8, leading to activation of downstream caspases and finally of the executioner caspase, caspase-3**.** These caspases are involved in the degradation of important cellular proteins as well as activation of caspase-activated DNAses that cleave mitochondrial DNA, ultimately leading to cell death. In addition, CHX enhances the induction of apoptosis via TNF-α by inhibition of new protein synthesis. One of the proteins that was first discovered to be essential for protection from TNF-mediated cell death is SOD2 (42, 43). Since this initial observation by Wong and Goeddel (42), numerous reports have demonstrated a role for SOD2 in protection from many apoptotic stimuli (21, 23, 26, 32, 39, 41). The antiapoptotic effects of SOD2 are attributed to its ability to remove $O_2^{\cdot-}$ at near diffusion-limiting rates. However, the role of ROS in protection from TNF-α–induced apoptosis is controversial. Several studies report that antioxidants can protect against TNF-α toxicity, whereas others demonstrate the opposite (2).

In this study, a series of well-characterized redox-engineered HT-1080 human fibrosarcoma cell lines were used to demonstrate that protection from TNF-mediated apoptosis is attributed to the ability of SOD2 to increase the steady-state production of H_2O_2. These studies unveil a unique mechanism for an antioxidant enzyme to initiate a protective prooxidant response.

METHODS AND MATERIALS

Reagents

Human TNF-α (R & D Systems), CHX, propidium iodide (PI), 3-amino 1,2,4-triazole (AT), H_2O_2, *N*-acetyl-L-cysteine (NAC), butylated hydroxytoluene (BHT), and bovine liver catalase were from Sigma, unless otherwise indicated. Dichlorodihydrofluorescein diacetate (DADCF), dihydroethidium (DHE), and JC-1 were from Molecular Probes. NP-40 substitute was purchased from USB Corporation and Sodium deoxycholate, from Acros Organics. Trolox was purchased from Oxis International; EDTA-free protease inhibitor cocktail tablets were purchased from Roche. The antibody against cleaved/ active caspase-3 was from Cell Signaling. Anti-procaspase-3 (CPP32) antibody and anti–poly-ADP ribose polymerase (PARP) antibodies were purchased from Pharmingen. CaspaTag Caspase detection kit was from Chemicon.

Cell lines and cell culture

All indicated cell lines were maintained in 25-cm^2 or 75-cm^2 flasks in MEM containing 10% fetal calf serum, 1,000 U/ml penicillin, 500 μg/ml streptomycin, and 1 mg/ml neomycin in a 37°C incubator under 5% CO_2. Constructions of the recombinant SOD2 and catalase plasmids and transfections were previously described in detail (3, 34), and their ability to alter the steady state production of H_2O_2 has been demonstrated in detail. In brief, the redox-engineered cell lines were generated in our laboratory from HT1080 human fibrosarcoma cells. The cell lines generated included cells that were transfected with control plasmid (Cmv), SOD2 targeted to the mitochondria (SOD2), and cells cotransfected with SOD2 directed to the cytosol (SOD2Cat) and catalase targeted to the cytosol (CmvCat).

Assessment of H_2O_2 and $O_2^{\cdot-}$

Cells were harvested with PBS-EDTA, washed, counted, pelleted, and resuspended in HBSS (Hanks buffered saline solution) to make a final count of 5×10^5 cells/ml. DHE or DADCF (Sigma) was added to make a final concentration of 10 μ*M*, and rate of oxidation of the dyes was monitored by FACS between 550 and 590 nm for DHE and 580 and 620 nm for DADCF for 300 s.

3-Amino 1, 2, 4-triazole–dependent inhibition of catalase to determine intracellular H_2O_2

Cells were treated with 20 m*M* aminotriazole (Sigma) for 1 h, resuspended in a final solution of 0.05 *M* potassium phosphate buffer (pH 7.0), sonicated, centrifuged, and supernatant was collected. Catalase activity was then measured based on the method of Claiborne (9). In brief, catalase activity was measured by using a kinetics-based spectrophotometric assay: 1 mg/ml of standard catalase at 1:100 dilutions is used to determine the working of the assay. A 5×10^{-3} *M* solution of H_2O_2 is prepared by mixing 0.15 ml of 30% H_2O_2 and 24.85 ml of 0.05 M potassium phosphate buffer, pH 7.0. Then 20 and 40 μl of the standard (bovine liver catalase) and samples are used for the assay. Then 500 μl of H_2O_2 is used for each reaction, and the final volume is adjusted to 1.5 ml by using the potassium

phosphate buffer. The absorbance is read at 240 nm, and rates are determined. Specific activity is then determined for each sample and adjusted to protein concentration, giving a value of units of enzyme activity per milligram protein.

Assessment of mitochondrial membrane potential as a measure of induction of apoptosis

Cells were treated with 0.3 ng/ml of TNF-α and 10 μg/ml of CHX for 16 h to induce apoptosis. After treatment, both floating and adherent cells were collected, pelleted, washed, and resuspended in PBS containing 2.5 μg/ml JC-1 dye (Molecular Probes). JC-1 dye was prepared in DMSO. Cells were kept in dark for 20 min, washed twice with PBS, and analyzed by flow cytometry (Becton-Dickinson). Excitation wavelength for JC-1: 490 nm; emission wavelength in the range of 530–590 nm. Change in mitochondrial potential was measured by the loss of red fluorescence.

Determining apoptotic cell population via sub-G1 analysis by flow cytometry

Flow cytometry was used to determine the population of apoptotic cells after TNF-α/CHX treatment. Cells were seeded in T-75 flasks, and on reaching 80% confluence, were treated with 0.3 ng/ml of TNF-α and 10 μg/ml of CHX for 8 h. After treatment, both floating cells and adherent cells were collected and spun at 1,500 rpm for 5 min. The pellet was washed once with 1× PBS, resuspended in 80% ice-cold ethanol, and stored at 4°C overnight. The cells were spun down and washed with 1× PBS and then resuspended in the staining solution consisting of 1× PBS, RNAse A, EDTA, and PI. The cells were incubated in the dark at 37°C for 30 min and then read in the FL-3 channel (excitation λ, 536 nm, and emission λ, 617 nm) of the BDFacsScan to determine the cell-cycle pattern of the population. The sub-G1 population represents the apoptotic cells.

Western blotting for caspase-3, active caspase-3, and PARP

The cells were treated for 4 or 8 h with 0.3 ng/ml of TNF-α and 10 μg/ml of CHX to determine the level of active caspase-3 in the control (Cmv) and SOD2 cell lines. A time-course experiment to determine the rate of disappearance of pro–caspase-3 was similarly performed by using anti–pro-Caspase-3 antibody. Both floating and adherent cells were collected after treatment and spun down at 1,500 rpm for 5 min. The pellet was washed in 1× PBS and then resuspended in lysis buffer (1× PBS, pH 7.4, 1% NP-40, 0.5% Sodium deoxycholate, and 0.1% SDS. Protease inhibitor tablets were added before use). Cell lysates were prepared by sonication. The lysates were spun at 10,000 rpm for 10 min at 4°C to remove cell debris. The supernatant was collected, and protein concentration determined. Lysates containing 40 μg denatured protein from treated and untreated cells were resolved on 12% SDS–polyacrylamide gel and electroblotted onto PDVF membranes. The membrane was blocked in 5% milk in 1× Tween-TBS for an hour at room temperature followed by incubation with antibody for active caspase-3 (1:1,000) overnight at 4°C. The membrane was washed 3 times for 10 min each with 1× Tween-TBS and then incubated with anti-rabbit antibody at 1:10,000 for an hour at room temperature. Anti–pro-caspase-3 (1:1,000) and anti-PARP (1:1,000) were used to determine the level of pro–caspase-3 and PARP in the cells. After incubation with the appropriate secondary antibody, the membrane was washed in 1× Tween-TBS 3 times for 10 min each. Detection was carried out by using a Pierce Femto Chemiluminescence kit.

Pan-caspase activity assay

The Caspa-Tag caspase activity kit from Chemicon was used to determine the levels of total caspase activity after treatment with TNF-α/CHX. Cells were treated with 0.3 ng/ml of TNF-α and 10 μg/ml of CHX for 8 h. After treatment, floating and adherent cells were collected and stained with CaspaTag as per the instructions of the kit for 30 min at 37°C. The cells were washed, resuspended in suspension buffer, and counterstained with PI provided with the kit. The cells were analyzed with flow cytometry. CaspaTag staining was read according to the manufacturer's instructions.

Statistics

Analysis of variance (ANOVA) with $\alpha = 0.05$ was used for processing the data. A two-sample *t* test was used as posttest unless otherwise indicated.

RESULTS

Overexpression of SOD2 increases intracellular H_2O_2 levels

Various redox-sensitive dyes were used to characterize the oxidative state of the redox-engineered cell lines and demonstrate that overexpression of SOD2 results in increased intracellular steady-state levels of H_2O_2. We used DADCF, a fluorophore widely used to measure intracellular H_2O_2 levels by FACS analysis. DADCF is readily taken up by cells and is cleaved into dichlorodihydrofluorescein, which is then oxidized to a highly fluorescent product, dichlorofluorescein. Although in the literature, DADCF oxidation is often used as a measure of H_2O_2 levels, the dye can be oxidized by other reactive oxygen and nitrogen species generated in the cell (25). However, in the presence of the H_2O_2-generating enzyme SOD, DADCF is efficiently oxidized by H_2O_2 generated by its activity. Measurement of the rate of DADCF oxidation in the different cell lines showed that SOD2 overexpression increased the rate of oxidation of the fluorophore compared with the control cells (Cmv), demonstrating that overexpression of SOD2 increases the oxidation of DADCF. Coexpression of cytosolic (SOD2Cat) that neutralizes H_2O_2 reduces the rate of oxidation of DADCF (Fig.1a). To prove that the increased oxidation of DADCF in the SOD2 cells was indeed due to an increase in intracellular H_2O_2, H_2O_2 was added externally to the cells in the presence of the fluorophore as a positive control. Addition of H_2O_2 to the cells lines showed an increase in DADCF oxidation (Fig.1b). Further to confirm that overexpression of SOD2 increases the intracellular H_2O_2 levels, the level of superoxide ($O_2^{\cdot -}$) was determined in the Cmv and SOD2 cells. Because SOD2 converts $O_2^{\cdot -}$ to H_2O_2, overexpression of SOD2 should result in an increase in H_2O_2

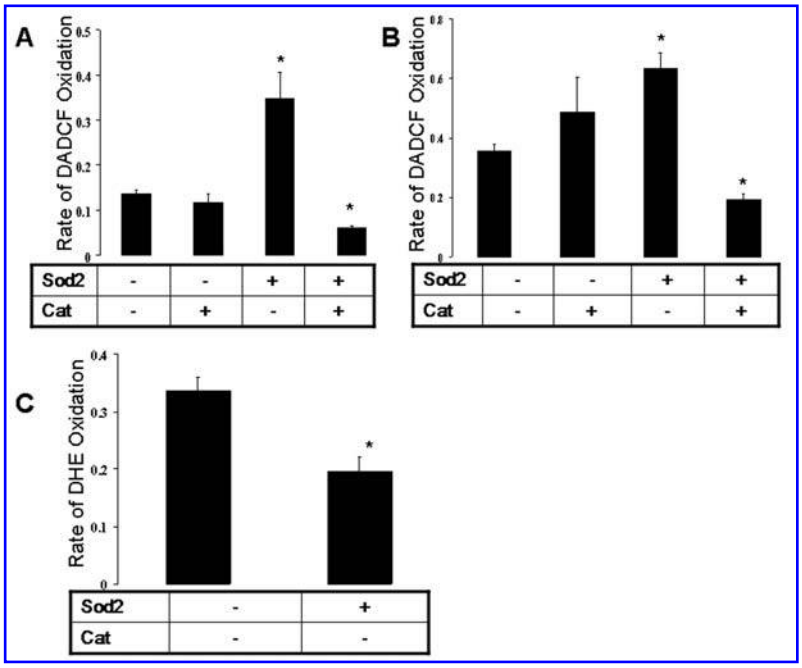

FIG. 1. Analysis of oxidation of redox-sensitive fluorophores in redox-engineered cell lines. (A) The rate of oxidation of the H_2O_2 specific fluorophore DADCF. DADCF was added to a final concentration of 10 μ*M*, and the rate of oxidation of the dye was measured by FACS at the appropriate wavelength for 300 s. Data are an average of three separate experiments ± SEM. *$p < 0.05$ when compared with the appropriate control group. (**B**) DADCF oxidation in the presence exogenous H_2O_2. Cells were treated as described earlier with the addition of 100 μM H_2O_2. (**C**) Rate of oxidation of the superoxide-specific fluorophore DHE. DHE was added to a final concentration of 10 μ*M*, and its rate of oxidation was measured as described earlier. Rate of oxidation in each case represents change in mean fluorescent intensity per second.

levels and a concomitant decrease in superoxide levels. Levels of intracellular $O_2^{\cdot -}$ were analyzed by using DHE, a superoxide specific fluorophore (4). The SOD2 cells showed a decrease in oxidation of DHE compared with Cmv, indicating that overexpression of SOD2 results in a decrease in levels of superoxide because of the enhanced dismutation activity of SOD2 (Fig. 1c).

In addition to the redox-sensitive dyes, we used a biochemical approach to demonstrate that SOD2 overexpression increases intracellular H_2O_2. The method is based on the determination of the rate of irreversible inactivation of catalase by amino 1, 2, 4-triazole (AT), as previously described (45). In the first step of its catalytic cycle, catalase is oxidized by one molecule of H_2O_2 to form the catalase intermediate compound I. Aminotriazole inactivates catalase by forming a covalent complex with compound I in a one-to-one stoichiometry:

$$H_2O_2 + \text{catalase} \rightarrow \text{compound I} \quad (1)$$

$$\text{Compound I} + \text{AT} \rightarrow \text{inactive catalase} \quad (2)$$

Thus, assuming that the concentration of AT is not rate limiting, the steady-state concentration of H_2O_2 can be estimated from the rate of catalase inactivation. This was determined empirically, and linearization was attained by plotting the natural log of catalase activity normalized to its activity at the start of the reaction (Fig. 2). The apparent pseudo first-order rate constant for catalase inhibition by AT in the two different cell lines was then determined from the slope of the linearizations. We found that the rate of inactivation of catalase was 1.6-fold greater in cells overexpressing SOD2 compared with the Cmv parent cells (0.92×10^{-3} *vs.* 1.53×10^{-3} per second), consistent with an increase in steady-state concentration of H_2O_2 on forced expression of SOD2.

A direct estimate of H_2O_2 steady-state concentrations in the two cell lines was determined by using a set of differential equation derived from Eq. 1 and 2, as previously described (45). Once solved, the steady-state concentration of H_2O_2 could be calculated from Eq. 3, assuming again that reactions 1 and 2 were irreversible and that aminotriazole was not rate limiting in the assay:

$$[H_2O_2] = k/k_1 \quad (3)$$

where k is the first-order rate constant determined empirically for catalase inactivation in the cell, and k_1 is the rate of

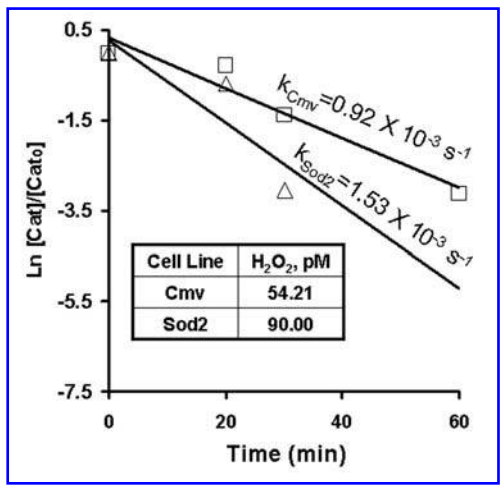

FIG. 2. Exponential decrease in catalase activity in Cmv and SOD2-overexpressing cells. Intracellular H_2O_2 levels were estimated in Cmv cells and SOD2-overexpressing cells by using aminotriazole-mediated inactivation of catalase. Data points were normalized by dividing with catalase activity measured at the start of the reaction, as described in Materials and Methods. See Result section for details.

compound I formation (1.7×10^7 M/s) (45). From the calculation from the experiments described in Fig. 2. the steady-state concentration of H_2O_2 in the SOD2-overexpressing cells was estimated at 90 p*M* compared to 54 p*M* in the parent Cmv cell line. Overall, these findings confirm that SOD2 overexpression does increase the intracellular levels of H_2O_2.

Increases in the SOD2-dependent production of H_2O_2 protects cells from TNF-α– induced cell death

The various cell lines were treated with TNF-α and CHX to induce apoptosis followed by fixation and PI staining to monitor DNA content. Sub-G_1 population represents the number of cells with haplodiploid nuclei, a characteristic of cells undergoing cell death by apoptosis (30). SOD2-overexpressing cells were resistant to TNF-α/CHX–induced apoptosis when compared with control cells (Fig. 3). The sensitivity to cell death was restored when catalase was coexpressed in the SOD2-overexpressing cell lines (SOD2Cat) (Fig. 3). CmvCat cells with the lowest levels of intracellular H_2O_2 were most sensitive to TNF-α/CHX–induced cell death. This suggests that the protective phenotype of the SOD2 is due to the increased steady-state levels of H_2O_2.

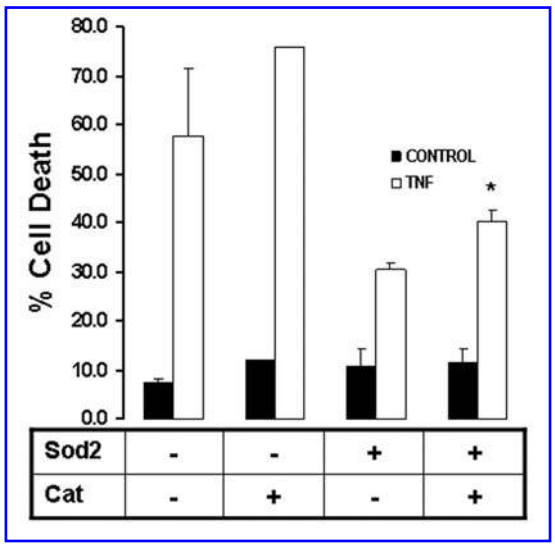

FIG. 3. SOD2-dependent resistance to TNF-α/CHX-induced apoptosis is reversed by catalase coexpression. Cells were treated with 0.3 ng/ml of TNF-α and 10 μg/ml of CHX for 8 h. After treatment, the floating and adherent cells were collected, pelleted, washed with 1× PBS, and fixed by using 80% ice-cold ethanol overnight at 4°C. The fixed cells were pelleted and stained with propidium iodide (PI) staining solution, as explained in Materials and Methods. Cell-cycle pattern for TNF-α/CHX–treated and untreated cells were read by using PI fluorescence in the red channel of the Becton-Dickinson flow cytometer. The sub-G1 population in each case was taken as an indicator of apoptosis. *$p < 0.05$ relative to SOD2 cells. Data are the average of three separate experiments ± SEM. SEM for the catalase overexpressors is too small to be visible.

SOD2-generated H_2O_2 protect cells from loss of mitochondrial membrane potential after TNF-α/CHX treatment

One of the hallmarks of cells undergoing apoptosis is the loss of mitochondrial membrane integrity, resulting in a decrease in mitochondrial membrane potential (36). The final outcome of mitochondrial disruption is release of cytochrome *c* and caspase activation. It is, however, possible that cytochrome *c* release can occur without any mitochondrial membrane depolarization. Recently it was demonstrated by Gilmore *et al.* (13) that cytosolic cytochrome *c* by itself can induce a caspase-dependent loss of mitochondrial membrane potential. These results show that, in intact cells, at a point downstream of the activation of caspase-3–like enzymes, cytochrome *c*–induced activation of caspases can exert a feedback effect on the mitochondria, leading to membrane depolarization, release of more cytochrome *c,* and amplification of the apoptotic cascade. In our system, we monitored the loss of membrane depolarization as well as caspase activation after 16 h of treatment. Membrane depolarization was evaluated with the potentiometric fluorophore JC-1. In cells that have not undergone membrane depolarization, JC-1 is distributed in both the cytoplasm as a monomer (green fluor) and in the mitochondria as an aggregate (red fluor) (33). Loss of mitochondrial membrane polarization (MMP) leads to dissipation of red fluorescence and retention of only fluorescence in the green channel. After treatment of the cells with both TNF-α/CHX, control cells lose their red fluorescence, whereas the SOD2-overexpressing cells are resistant to this loss (Fig. 4a). The resistance to loss of MMP was reversed by coexpression of catalase (SOD2Cat). In addition, overexpression of cytosolic catalase alone in our control cells (CmvCat) results in an increased loss of mitochondrial membrane potential with TNF-α/CHX treatment. This suggests that H_2O_2 protects SOD2-overexpressing cells from MMP loss and confers resistance to TNF-α/CHX–induced apoptosis.

TNF-α/CHX treatment leads to caspase-3 activation and cleavage of its downstream target, PARP

To confirm that TNF-α/CHX treatment induces cell death via apoptosis, levels of pro–caspase-3, active caspase-3, and poly-ADP ribose polymerase (PARP) were determined. The Cmv and SOD2 cells were treated with or without TNF-α/CHX for 4 or 8 h. After treatment, the adherent and floating cells were collected, and cell lysates were used to perform a Western blot for active caspase-3. At both 4 and 8 h, the Cmv cells had higher levels of active caspase-3 (seen as 17/19-kDa bands) compared with the SOD2 cells (Fig. 5a). Thus, cell death induced after TNF-α/CHX treatment does involve apoptosis. We also determined the levels of cleaved PARP (85Kd band), a downstream target of active caspase-3. High levels of active caspase-3 in the Cmv cells corresponded with increased levels of cleaved PARP compared with the SOD2 cells (Fig. 5a, lower panel). The disappearance of pro–caspase-3 as readout of apoptosis induction was also determined (Fig. 5b). Results show that with time, a significant decrease in the level of pro–caspase-3 occurs in the Cmv cells

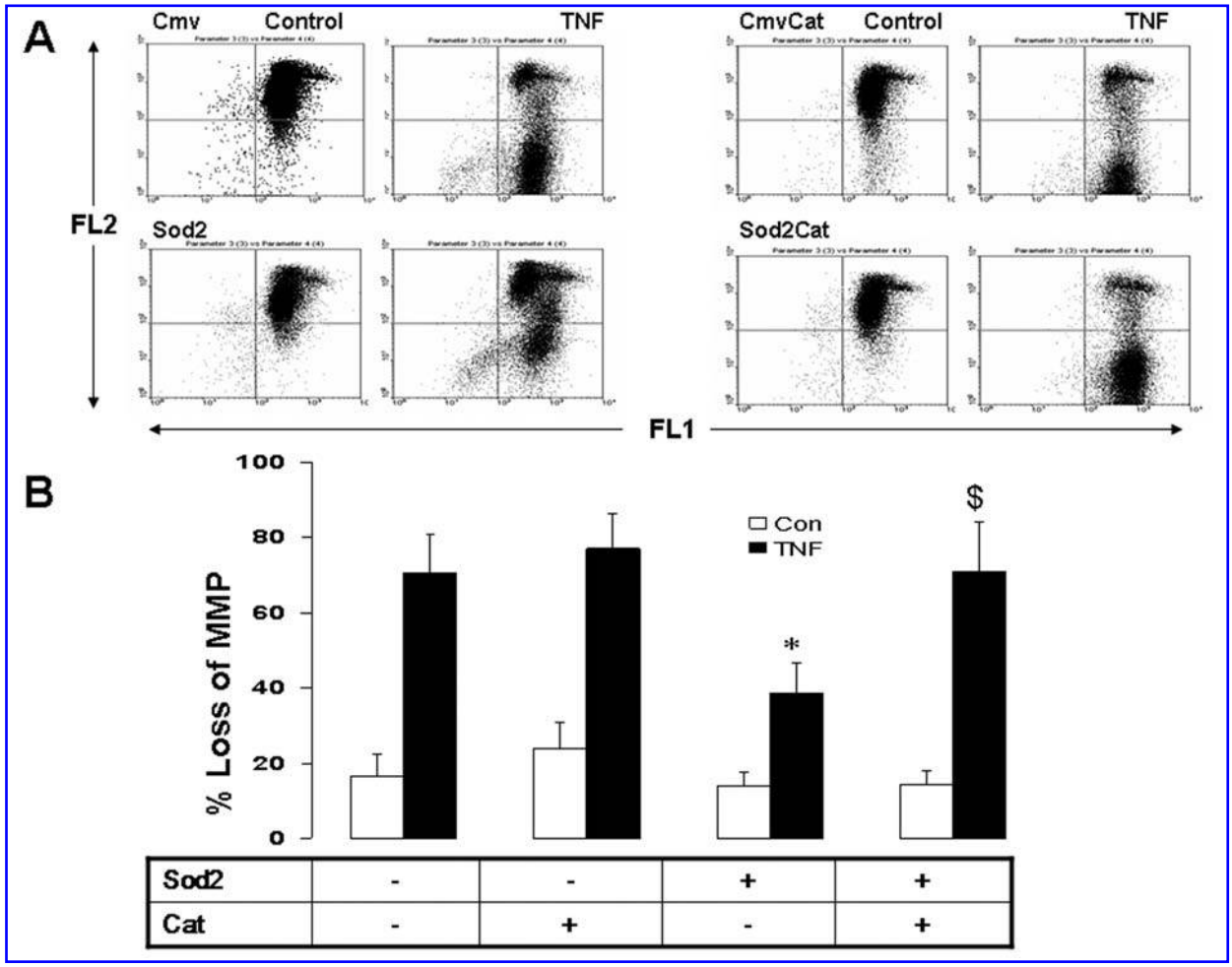

FIG. 4. SOD2-dependent inhibition of TNF-α/CHX–induced loss of mitochondrial membrane potential is prevented by catalase coexpression. (**A**) Representative histogram analysis of mitochondrial membrane potential (MMP) as detected by JC-1. The *x* axis (FL1) indicates the green fluorescence intensity of JC-1 monomer, and the *y* axis (FL2) indicates the red fluorescence intensity of J aggregates. Cells were either treated with 0.3 ng/ml TNF-α and 10 μg/ml CHX for 16 h or left untreated and analyzed for JC-1 fluorescence, as described in Materials and Methods. (**B**) Quantitative analysis of data from **A**. Numbers of cells in upper and lower right hand quadrants were counted and normalized to total cells. Data were plotted as a bar graph showing various cell lines and the number of cells that have lost MMP. Data are the average of four separate experiments ± SEM. * or $$p < 0.05$ as compared with Cmv or SOD2 treated with TNF-α, respectively.

compared with the SOD2 cells. The decrease in level of pro–caspase-3 could be restored in the SOD2Cat-coexpressing cells, again showing that the protection seen in response to SOD2 overexpression is H_2O_2 dependent. We also confirmed that disappearance of pro–caspase-3 is associated with the increased cleavage of PARP. Decreased levels of pro–caspase-3 in the Cmv and the SOD2Cat cells corresponded with an increase in the levels of cleaved PARP compared with the SOD2 cells, confirming that caspase-3 is active in these cells after TNF-α/CHX treatment. In addition to caspase-3, we also determined the levels of pan-caspase activity in the cell lines after TNF-α/CHX treatment. The Cmv cells had an overall high level of active caspases after treatment, which was significantly reduced after SOD2 overexpression. The level of active caspases in the SOD2 overexpressers was restored to that of the control cells after catalase coexpression (Fig. 6). These findings indicate that increases in the steady-state levels of H_2O_2 protect cells from TNF-α/CHX–induced caspase-dependent cell death.

Lipid peroxides are not involved in the protection of the SOD2 cells against apoptosis

Lipid hydroperoxides are generated as peroxidation products of long-chain lipids in cells undergoing oxidative stress and have emerged as important signaling intermediates (14, 15). Because SOD2 overexpression increases oxidant production, it was important to determine whether lipid hydroperoxides were involved in mediating any of the anti-apoptotic affects associated with its overexpression. The SOD2-overexpressing cells were treated with TNF-α and CHX in combination with or without the lipid hydroperoxide scavengers/inhibitors trolox (100 μ*M*), butylated hydroxytoluene (BHT) (25 μ*M*), or desferoxamine (DFX) (100 μ*M*).

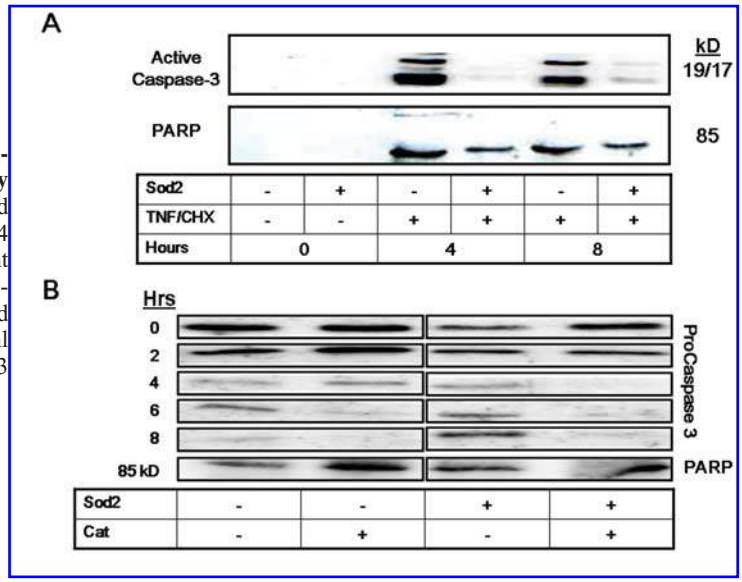

FIG. 5. TNF-α-mediated caspase activation is inhibited by SOD2 overexpression and attenuated by coexpression of catalase. (**A**) Cells were treated with 0.3 ng/ml TNF-α and 10 μg/ml CHX for either 4 or 8 h. Equal amount of protein from the supernatant was resolved on SDS-PAGE and probed for active caspase-3 or PARP by Western blotting. (**B**) The indicated cells were treated with 0.3 ng/ml TNF-α and 10 μg/ml CHX for varying periods, and levels of pro–Caspase-3 and PARP were determined by Western blotting.

After treatment, the loss of MMP and caspase-3 activity was measured in the various cell lines. In Fig. 7a and b, SOD2-overexpressig cells treated with the lipid hydroperoxide scavengers/inhibitors showed a small increase in the number of cells that lose mitochondrial membrane potential but not to the degree that was observed in response to catalase coexpression (Fig. 4). These findings suggest that inhibition of the loss of MMP in response to SOD2 overexpression is not attributed to the production of lipid hydroperoxides. The level of caspase-3 activation in SOD2 cells in the presence and absence of these scavengers was also determined after TNF-α/CHX treatment. A slight increase in the levels of active caspase-3 was noted in the SOD2 cells after treatment with TNF-α/CHX in the presence of the inhibitors/scavengers (Fig. 8). However, the level of activation was much less compared with that seen in Cmv cells. This suggests that lipid peroxides play a minor role, if any, in the protection of the SOD2-overexpressing cells against loss of MMP and caspase-3 activation.

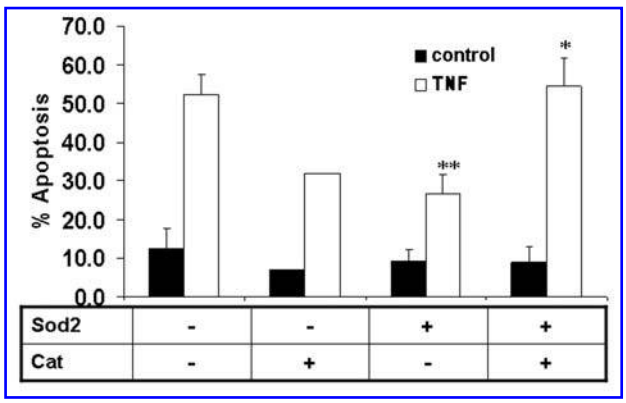

FIG. 6. CaspaTag assay to determine percentage of apoptotic cells based on level of caspase activity and propidium iodide (PI) permeability. Cells were treated with 0.3 ng/ml of TNF-a and 10 μg/ml of cycloheximide (CHX) for 8 h, followed by incubation with fluorescent pan-caspase substrate and PI. Fluorescence was measured in FL-1 and FL-2 channels on a BD Flowcytometer. Dual positive populations of cells were taken as apoptotic. Data are the average of three separate experiments ± SEM. SEM for the catalase overexpressors is too small to be visible. $^{**}p < 0.005$. $^{*}p < 0.05$ relative to the control untreated or SOD2-overexpressing cell lines, respectively.

DISCUSSION

SOD2, a mitochondrial antioxidant enzyme, is responsible for dismutation of $2H^+ + 2O_2^{\cdot -}$ to $H_2O_2 + O_2$. However, the ability of SOD2 to generate H_2O_2 when overexpressed has been controversial. Our laboratory previously reported the generation of a group of redox-engineered cell lines from HT1080 human fibrosarcoma cells that overexpress or coexpress SOD2 and catalase (34). Different approaches have been taken to demonstrate that overexpression of SOD2 is capable of increasing the steady-state levels of H_2O_2. In this study, we demonstrated that various redox-sensitive fluorophores modulate their oxidation state based on antioxidant enzyme overexpression. In all cases using redox-sensitive fluorescent dyes that are responsive to H_2O_2-dependent oxidation, SOD2 overexpression leads to an increase in fluor oxidation (fluorescence), which is reversed by catalase coexpression (34). When $O_2^{\cdot -}$-responsive fluorophores were used, SOD2 inhibited their basal rate of oxidation that was unaffected by catalase overexpression. Using the AT-dependent inhibition of the complex-I form of catalase, we demonstrated that SOD2 overexpression can increase the steady-state production of H_2O_2. These findings suggest that with the appropriate controls, redox-sensitive fluorophores can be used with reliability to monitor, qualitatively, intracellular $O_2^{\cdot -}$ and H_2O_2 levels. Furthermore, by coupling the use of the redox-sensitive fluorophores and AT-dependent inhibition of catalase, we demonstrated that SOD2 overexpression leads to an increase in the steady-state production of H_2O_2.

SOD2 overexpression or its inducible upregulation has long been established as a physiologic outcome to the augmented

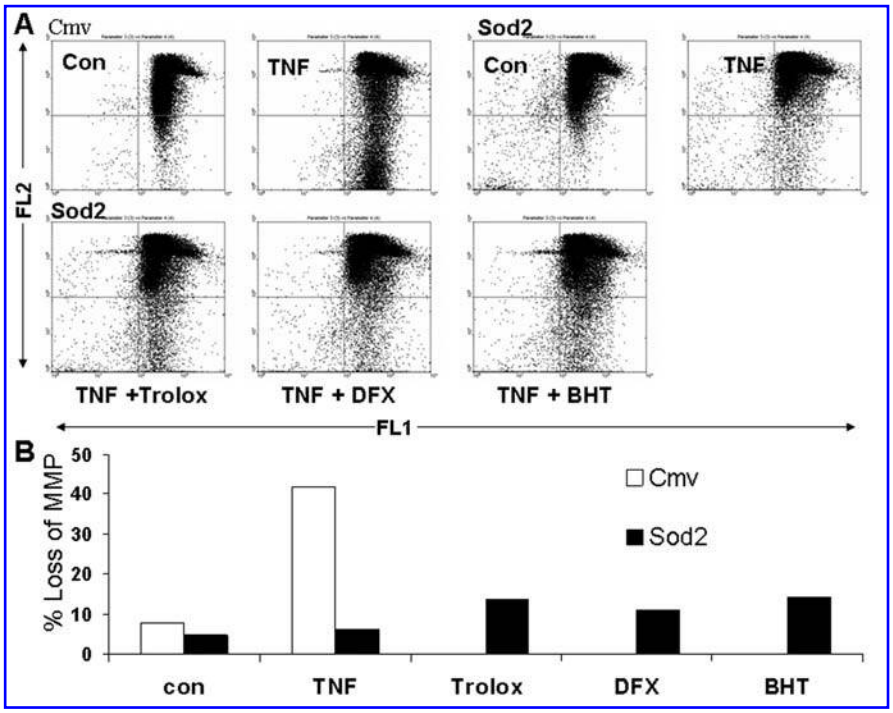

FIG. 7. Lipid hydroperoxide scavengers do not reverse the SOD2-dependent inhibition of MMP loss. (**A**) Cells were treated as described in Fig. 4 with or without 100 μ*M* trolox, 100 μ*M* desferoxamine, or 25 μ*M* butylated hydroxytoluene, and MMP was monitored by using JC-1. (**B**) Data from A were quantified as described in Fig. 4.

production of $O_2^{\cdot -}$ in response to numerous apoptotic stimuli (27). The protective role of SOD2 during apoptosis is attributed to its ability efficiently to dismute $O_2^{\cdot -}$ generated in response to the stimuli in question. Many aggressive tumors show increased SOD2 expression and activity (16) that, based on our observations, should increase intracellular H_2O_2 levels. Interestingly, tumors with increased SOD2 levels are also resistant to apoptosis induction (24, 26) and may be an underlying reason for the reason that these cells survive in the body for prolonged periods even under unfavorable conditions. Literature reports suggest that H_2O_2 might play a protective role against apoptosis (8, 37, 38). Our findings also support the idea that the intracellular production of H_2O_2 protects against apoptosis. TNF-α was first demonstrated to be a potent inducer of SOD2 expression by Wong and Goeddel (43). SOD2 was then shown to be essential for survival from TNF-mediated cell death. The use of TNF in combination with CHX inhibits synthesis of any new proteins in cells, and any protection from this mode of cell killing is attributed to proteins that are already present in the cell. Thus, SOD2 was shown to be a major factor responsible for protection from apoptotic death. Since this initial discovery, many of the molecular signals that control apoptosis have been defined. The present findings indicate that SOD2 protects from TNF-mediated apoptosis by increasing the steady-state production of H_2O_2, which in turn restricts various facets of the apoptotic process. The exact mechanism of how H_2O_2 restricts apoptosis has not been defined. Our studies indicate that H_2O_2 blocks the MMP loss, prevents caspase activation, PARP cleavage, and the accumulation of hypodiploid DNA content. The loss of MMP and caspase activation is a relatively early apoptotic event, whereas PARP cleavage and increase in hypodiploid DNA occur downstream (22). SOD2's ability to inhibit caspase activation is likely the primary reason for restricting the programmed cell death. Brown and co-workers (6) have shown that H_2O_2 can oxidize critical active-site cysteines, and this mode of caspase inactivation may also occur in response to the SOD2-dependent increase in H_2O_2 levels (6). It is intriguing to hypothesize that mechanisms to inhibit SOD2 activity might be successful in potentiating apoptotic cell death. Alternatively, H_2O_2 detoxification might be used to enhance apoptotic cell death either in cells with relatively high levels of SOD2 or with a high basal metabolic production of H_2O_2.

Lipid hydroperoxides have been shown to be generated in response to SOD2 overexpression. Thus, it was important to determine whether the protective effect against apoptosis was due to generation of lipid hydroperoxides. By using a number of po-

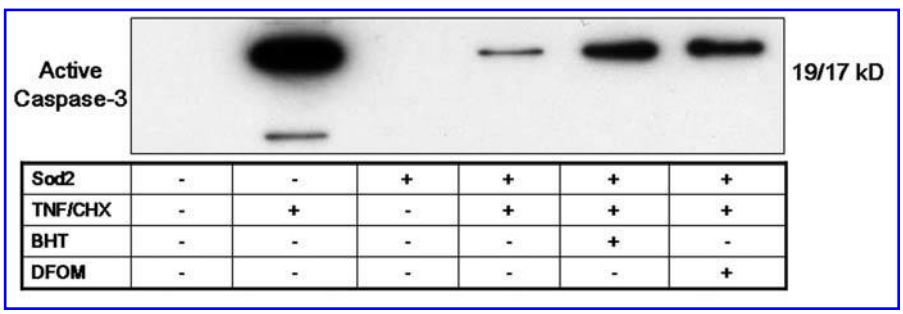

FIG. 8. SOD2-dependent inhibition of TNF-mediated caspase activation is not reversed by lipid hydroperoxide scavengers. Control and SOD2-overexpressing cells were treated as described in Fig. 7, and an equal amount of protein from the supernatant was resolved on a SDS-PAGE and probed for active caspase-3.

tent lipid hydroperoxide inhibitors, we demonstrated that little effect was found on the SOD2-dependent inhibition of caspase activation or loss of MMP. Although the SOD2-overexpressing cells showed some increase in loss of MMP and increase in levels of active caspase-3 after TNF-α/CHX in combination with the lipid hydroperoxide inhibitor, the levels were much lower than in control cells. This suggests that lipid hydroperoxides might play a minor role in the SOD2-dependent inhibition of apoptosis. However, the major protective molecule seems to be H_2O_2 because the effects can be reversed in all cases by coexpression of catalase, as seen in the SOD2Cat cells.

The present data demonstrate that mitochondrial H_2O_2 plays a protective role in TNF-α/CHX–induced apoptosis. The protection afforded here does not require *de novo* protein synthesis and could be directly attributed to the effect of H_2O_2. This contradicts the well-established idea that H_2O_2 is a proapoptotic molecule. The exact molecular targets that are sensitive to the SOD2-dependent production of H_2O_2 have yet to be determined. It is likely that the localized production of H_2O_2 in the mitochondrial microenvironment will oxidize and alter function of key pro- or antiapoptotic molecules, leading to their inhibition or activation, respectively. Brown and coworkers (6) have shown that the active site cysteines of both caspase-3 and 8 are sensitive to reversible H_2O_2-dependent inactivation (6). Our findings clearly demonstrate that the TNF-dependent caspase-3 activation is inhibited by SOD2 overexpression and rescued by coexpression of catalase. Thus, the caspases are ideal candidates for inactivation by SOD2-generated H_2O_2. In addition, we previously demonstrated that the prosurvival signal Akt is indirectly activated by the SOD2-dependent production of H_2O_2 by oxidative inactivation of its antagonist, the dual-specificity phosphatase, PTEN. Loss of SOD2 expression has also long been established to be associated with a variety of tumor types (31). However, in recent years, a number of studies have linked increases in SOD2 expression to a more malignant and metastatic phenotype (18, 19, 29, 35). It has recently been reported that combinatorial antisense treatments targeted at both SOD2 and bcl-2 sensitize highly resistant metastatic tumor cells to apoptosis in response to chemotherapeutic drugs and TNF (5). Our findings also support the idea that the high SOD2 expression in malignant cells can enhance their survival in response to apoptotic stimuli. Thus, strategies targeted at decreasing SOD2 expression in metastatic lesions may allow their effective elimination.

ACKNOWLEDGMENTS

Research described in this article was supported, in part, by Philip Morris USA Inc. and Philip Morris International, and PHS grants CA77068 and CA095011 to J.A.M. and an NIH Predoctoral Fellowship AI49822 to K.M.C.

ABBREVIATIONS

Asp, Aspartate; AT, 1-amino-1,2,4-triazole; BHT, butylated hydroxytoluene; CHX, cycloheximide; DADCF, 2′,7′-dichlorodihydrofluorescein diacetate; DHE, dihydroethidium; DFX, desferrioxamine; DMSO, dimethylsulfoxide; DNA, deoxyribonucleic acid; EDTA, ethylenediaminetetraacetic acid; FACS, fluorescence-activated cell sorter; HBSS, Hanks buffered saline solution; H_2O_2, hydrogen peroxide; JC-1, 5,5′,6,6′-tetrachloro-1,1′,3,3′-tetraethylbenzimidazolylcarbocyanine iodide/chloride; MEM, minimum essential medium; MMP, mitochondrial membrane potential; NAC, *N*-acetyl cysteine; NP-40, nonidet P40; $O_2^{\bullet -}$, superoxide; PARP, poly-ADP ribose polymerase; PBS, phosphate-buffered saline; PI, propidium iodide; PTEN, phosphatase and tensin homolog on chromosome 10; RNAse A, ribonuclease A; ROS, reactive oxygen species; SDS, SODium dodecylsulfate; SOD2, manganese superoxide dismutase; TBS, Tris-buffered saline; TNF-α, tumor necrosis factor-α.

REFERENCES

1. Adams JM. Ways of dying: multiple pathways to apoptosis. *Genes Dev* 17: 2481–2495, 2003.
2. Bai J and Cederbaum AI. Overexpression of catalase in the mitochondrial or cytosolic compartment increases sensitivity of HepG2 cells to tumor necrosis factor-alpha -induced apoptosis. *J Biol Chem* 275: 19241–19249, 2000.
3. Bai J, Rodriguez AM, Melendez JA, and Cederbaum AI. Overexpression of catalase in cytosolic or mitochondrial compartment protects HepG2 cells against oxidative injury. *J Biol Chem* 274: 26217–26224, 1999.
4. Becker LB, vanden Hoek TL, Shao ZH, Li CQ, and Schumacker PT. Generation of superoxide in cardiomyocytes during ischemia before reperfusion. *Am J Physiol* 277: H2240–H2246, 1999.
5. Benlloch M, Mena S, Ferrer P, Obrador E, Asensi M, Pellicer JA, Carretero J, Ortega A, and Estrela JM. Bcl-2 and Mn-SOD antisense oligodeoxynucleotides and a glutamine-enriched diet facilitate elimination of highly resistant B16 melanoma cells by tumor necrosis factor-α and chemotherapy. *J Biol Chem* 281: 69–79, 2006.
6. Borutaite V and Brown GC. Caspases are reversibly inactivated by hydrogen peroxide. *FEBS Lett* 500: 114–118, 2001.
7. Boveris A and Chance B. The mitochondrial generation of hydrogen peroxide: general properties and effect of hyperbaric oxygen. *Biochem J* 134: 707–716, 1973.
8. Butts BD, Kwei KA, Bowden GT, and Briehl MM. Elevated basal reactive oxygen species and phospho-Akt in murine keratinocytes resistant to ultraviolet B-induced apoptosis. *Mol Carcinog* 37: 149–157, 2003.
9. Claiborne A. Catalase activity. In: Greenwald RA (ed). *CRC Handbook of Methods for Oxygen Radical Research*. Boca Raton, Fl: CRC Press, 1985, pp 283–284.
10. Clement MV, Ponton A, and Pervaiz S. Apoptosis induced by hydrogen peroxide is mediated by decreased superoxide anion concentration and reduction of intracellular milieu. *FEBS Lett* 440: 13–18, 1998.
11. Forrest VJ, Kang YH, McClain DE, Robinson DH, and Ramakrishnan N. Oxidative stress-induced apoptosis prevented by trolox. *Free Radic Biol Med* 16: 675–684, 1994.

12. Gate L, Paul J, Ba GN, Tew KD, and Tapiero H. Oxidative stress induced in pathologies: the role of antioxidants. *Biomed Pharmacother* 53: 169–180, 1999.
13. Gilmore KJ, Quinn HE, and Wilson MR. Pinocytic loading of cytochrome c into intact cells specifically induces caspase-dependent permeabilization of mitochondria: evidence for a cytochrome c feedback loop. *Cell Death Differ* 8: 631–639, 2001.
14. Girotti AW. Lipid hydroperoxide generation, turnover, and effector action in biological systems. *J Lipid Res* 39: 1529–1542, 1998.
15. Girotti AW and Kriska T. Role of lipid hydroperoxides in photo-oxidative stress signaling. *Antioxid Redox Signal* 6: 301–310, 2004.
16. Hu Y, Rosen DG, Zhou Y, Feng L, Yang G, Liu J, and Huang P. Mitochondrial manganese-superoxide dismutase expression in ovarian cancer: role in cell proliferation and response to oxidative stress. *J Biol Chem* 280: 39485–39492, 2005.
17. Igney FH and Krammer PH. Death and anti-death: tumour resistance to apoptosis. *Nat Rev Cancer* 2: 277–288, 2002.
18. Janssen AM, Bosman CB, Kruidenier L, Griffioen G, Lamers CB, van Krieken JH, van de Velde CJ, and Verspaget HW. Superoxide dismutases in the human colorectal cancer sequence. *J Cancer Res Clin Oncol* 125: 327–335, 1999.
19. Janssen AM, Bosman CB, van Duijn W, Oostendorp-van de Ruit MM, Kubben F. J, Griffioen G, Lamers CB, van Krieken JH, van de Velde CJ, and Verspaget HW. Superoxide dismutases in gastric and esophageal cancer and the prognostic impact in gastric cancer. *Clin Cancer Res* 6: 3183–3192, 2000.
20. Kanduc D, Mittelman A, Serpico R, Sinigaglia E, Sinha AA, Natale C, Santacroce R, Di Corcia MG, Lucchese A, Dini L, Pani P, Santacroce S, Simone S, Bucci R, and Farber E. Cell death: apoptosis versus necrosis. *Int J Oncol* 21: 165–170, 2002.
21. Kops GJ, Dansen TB, Polderman PE, Saarloos I, Wirtz KW, Coffer PJ, Huang TT, Bos JL, Medema RH, and Burgering BM. Forkhead transcription factor FOXO3a protects quiescent cells from oxidative stress. *Nature* 419: 316– 321, 2002.
22. Krilleke D, Ucur E, Pulte D, Schulze-Osthoff K, Debatin KM, and Herr I. Inhibition of JNK signaling diminishes early but not late cellular stress-induced apoptosis. *Int J Cancer* 107: 520–527, 2003.
23. Li N, Ragheb KE, Lawler G, Sturgis J, Rajwa B, Melendez JA, and Robinson JP. Mitochondrial complex I inhibitor rotenone induces apoptosis through enhancing mitochondrial reactive oxygen species production. *J Biol Chem* 2002.
24. Liu Y, Borchert GL, Donald SP, Surazynski A, Hu CA, Weydert CJ, Oberley LW, and Phang JM. MnSOD inhibits proline oxidase-induced apoptosis in colorectal cancer cells. *Carcinogenesis* 26: 1335–1342, 2005.
25. Lufrano M and Balazy M. Interactions of peroxynitrite and other nitrating substances with human platelets: The role of glutathione and peroxynitrite permeability. *Biochem Pharmacol* 65: 515–523, 2003.
26. Manna SK, Zhang HJ, Yan T, Oberley LW, and Aggarwal BB. Overexpression of manganese superoxide dismutase suppresses tumor necrosis factor-induced apoptosis and activation of nuclear transcription factor-kappaB and activated protein-1. *J Biol Chem* 273: 13245–13254, 1998.
27. Motoyama S, Minamiya Y, Saito S, Saito R, Matsuzaki I, Abo S, Inaba H, Enomoto K, and Kitamura M. Hydrogen peroxide derived from hepatocytes induces sinusoidal endothelial cell apoptosis in perfused hypoxic rat liver. *Gastroenterology* 114: 153–163, 1998.
28. Motoyama S, Minamiya Y, Saito S, Saito R, Matsuzaki I, Abo S, Inaba H, Enomoto K, and Kitamura M. Hydrogen peroxide derived from hepatocytes induces sinusoidal endothelial cell apoptosis in perfused hypoxic rat liver. *Gastroenterology* 114: 153–163, 1998.
29. Nelson KK, Ranganathan AC, Mansouri J, Rodriguez AM, Providence KM, Rutter JL, Pumiglia K, Bennett JA, and Melendez JA. Elevated SOD2 activity augments matrix metalloproteinase expression: evidence for the involvement of endogenous hydrogen peroxide in regulating metastasis. *Clin Cancer Res* 9: 424–432, 2003.
30. Nicoletti I, Migliorati G, Pagliacci MC, Grignani F, and Riccardi C. A rapid and simple method for measuring thymocyte apoptosis by propidium iodide staining and flow cytometry. *J Immunol Methods* 139: 271–279, 1991.
31. Oberley LW and Buettner GR. Role of superoxide dismutase in cancer: a review. *Cancer Res* 39: 1141–1149. 1979.
32. Pani G, Bedogni B, Anzevino R, Colavitti R, Palazzotti B, Borrello S, and Galeotti T. Deregulated manganese superoxide dismutase expression and resistance to oxidative injury in p53-deficient cells. *Cancer Res* 60: 4654–4660, 2000.
33. Reers M, Smiley ST, Mottola-Hartshorn C, Chen A, Lin M, and Chen LB. Mitochondrial membrane potential monitored by JC-1 dye. *Methods Enzymol* 260:406–417, 1995.
34. Rodriguez AM, Carrico PM, Mazurkiewicz JE, and Melendez JA. Mitochondrial or cytosolic catalase reverses the MnSOD-dependent inhibition of proliferation by enhancing respiratory chain activity, net ATP production, and decreasing the steady state levels of H_2O_2. *Free Radic Biol Med* 29: 801–813, 2000.
35. Schadendorf D, Zuberbier T, Diehl S, Schadendorf C, and Czarnetzki BM. Serum manganese superoxide dismutase is a new tumour marker for malignant melanoma. *Melanoma Res* 5: 351–353, 1995.
36. Susin SA, Zamzami N, and Kroemer G. Mitochondria as regulators of apoptosis: Doubt no more. *Biochim Biophys Acta* 1366: 151–165, 1998.
37. Suzaki Y, Yoshizumi M, Kagami S, Koyama AH, Taketani Y, Houchi H, Tsuchiya K, Takeda E, and Tamaki T. Hydrogen peroxide stimulates c-Src-mediated big mitogen-activated protein kinase 1 (BMK1) and the MEF2C signaling pathway in PC12 cells: potential role in cell survival following oxidative insults. *J Biol Chem* 277: 9614–9621, 2002.
38. Takada Y, Hachiya M, Park SH, Osawa Y, Ozawa T, and Akashi M. Role of reactive oxygen species in cells overexpressing manganese superoxide dismutase: mechanism for induction of radioresistance. *Mol Cancer Res* 1: 137–146, 2002.
39. Tanaka H, Matsumura I, Ezoe S, Satoh Y, Sakamaki T, Albanese C, Machii T, Pestell RG, and Kanakura Y. E2F1 and

c-Myc potentiate apoptosis through inhibition of NF-kappaB activity that facilitates MnSOD-mediated ROS elimination. *Mol Cell* 9: 1017–1029, 2002.
40. Uberti D, Yavin E, Gil S, Ayasola KR, Goldfinger N, and Rotter V. Hydrogen peroxide induces nuclear translocation of p53 and apoptosis in cells of oligodendroglia origin. *Brain Res Mol Brain Res* 65: 167–175, 1999.
41. Wong GHW. Protective roles of cytokines against radiation: induction of mitochondrial MnSOD. *Biochim Biophys Acta* 1271: 205–209, 1995.
42. Wong GHW, Elwell JH, Oberley LW, and Goeddel DV. Manganous superoxide dismutase is essential for cellular resistance to cytotoxicity of tumor necrosis factor. *Cell* 58: 923–931, 1989.
43. Wong GHW and Goeddel DV. Induction of manganous superoxide dismutase by tumor necrosis factor: possible protective mechanism. *Science* 242: 941–944. 1988.
44. Wright SC, Kumar P, Tam AW, Shen N, Varma M, and Larrick JW. Apoptosis and DNA fragmentation precede TNF-induced cytolysis in U937 cells. *J Cell Biochem* 48: 344–355, 1992.
45. Yusa T, Beckman JS, Crapo JD, and Freeman BA. Hyperoxia increases H_2O_2 production by brain in vivo. *J Appl Physiol* 63: 353–358, 1987.

Address reprint requests to:
Center for Immunology and Microbial Disease MC151
Albany Medical College
47, New Scotland Ave.
Albany, NY 12208

E-mail: melenda@mail.amc.edu

Date of first submission to ARS Central, January 25, 2006; date of acceptance, February 7, 2006.

This article has been cited by:

1. Kristine Ansenberger-Fricano, Douglas da Silva Ganini, Mao Mao, Saurabh Chatterjee, Shannon Dallas, Ronald P. Mason, Krisztian Stadler, Janine H. Santos, Marcelo G. Bonini. 2012. The peroxidase activity of mitochondrial superoxide dismutase. *Free Radical Biology and Medicine* . [CrossRef]
2. Arseniy E. Yuzhalin, Anton G. Kutikhin. 2012. Inherited variations in the SOD and GPX gene families and cancer risk. *Free Radical Research* 1-19. [CrossRef]
3. Zhi Xu, Haixia Zhu, John M. Luk, Dongmei Wu, Dongying Gu, Weida Gong, Yongfei Tan, Jianwei Zhou, Jinhai Tang, Zhengdong Zhang, Meilin Wang, Jinfei Chen. 2012. Clinical significance of SOD2 and GSTP1 gene polymorphisms in Chinese patients with gastric cancer. *Cancer* n/a-n/a. [CrossRef]
4. Yuewei Sheng, Troy A. Stich, Kevin Barnese, Edith B. Gralla, Duilio Cascio, R. David Britt, Diane E. Cabelli, Joan Selverstone Valentine. 2011. Comparison of Two Yeast MnSODs: Mitochondrial Saccharomyces cerevisiae versus Cytosolic Candida albicans. *Journal of the American Chemical Society* 111130135723001. [CrossRef]
5. Edith Lubos , Joseph Loscalzo , Diane E. Handy . 2011. Glutathione Peroxidase-1 in Health and Disease: From Molecular Mechanisms to Therapeutic Opportunities. *Antioxidants & Redox Signaling* **15**:7, 1957-1997. [Abstract] [Full Text HTML] [Full Text PDF] [Full Text PDF with Links]
6. Jaya Dasgupta, Supriya Kar, Rong Liu, Joy Joseph, Balaraman Kalyanaraman, S. James Remington, Ceshi Chen, J. Andres Melendez. 2010. Reactive oxygen species control senescence-associated matrix metalloproteinase-1 through c-Jun-N-terminal kinase. *Journal of Cellular Physiology* **225**:1, 52-62. [CrossRef]
7. A. Mesquita, M. Weinberger, A. Silva, B. Sampaio-Marques, B. Almeida, C. Leao, V. Costa, F. Rodrigues, W. C. Burhans, P. Ludovico. 2010. Caloric restriction or catalase inactivation extends yeast chronological lifespan by inducing H2O2 and superoxide dismutase activity. *Proceedings of the National Academy of Sciences* **107**:34, 15123-15128. [CrossRef]
8. Samar M. Hammad, Waleed O. Twal, Jeremy L. Barth, Kent J. Smith, Antonio F. Saad, Gabriel Virella, W. Scott Argraves, Maria F. Lopes-Virella. 2009. Oxidized LDL immune complexes and oxidized LDL differentially affect the expression of genes involved with inflammation and survival in human U937 monocytic cells. *Atherosclerosis* **202**:2, 394-404. [CrossRef]
9. A. Rodriguez-Caballero, A. C. Garcia-Montero, P. Barcena, J. Almeida, F. Ruiz-Cabello, M. D. Tabernero, P. Garrido, S. Munoz-Criado, Y. Sandberg, A. W. Langerak, M. Gonzalez, A. Balanzategui, A. Orfao. 2008. Expanded cells in monoclonal TCR- +/CD4+/NKa+/CD8-/+dim T-LGL lymphocytosis recognize hCMV antigens. *Blood* **112**:12, 4609-4616. [CrossRef]
10. K. Yaegaki, W. Qian, T. Murata, T. Imai, T. Sato, T. Tanaka, T. Kamoda. 2008. Oral malodorous compound causes apoptosis and genomic DNA damage in human gingival fibroblasts. *Journal of Periodontal Research* **43**:4, 391-399. [CrossRef]
11. Christopher I. van de Wetering, Mitchell C. Coleman, Douglas R. Spitz, Brian J. Smith, C. Michael Knudson. 2008. Manganese superoxide dismutase gene dosage affects chromosomal instability and tumor onset in a mouse model of T cell lymphoma. *Free Radical Biology and Medicine* **44**:8, 1677-1686. [CrossRef]
12. Kang-Beom Kwon, Byung-Hyun Park, Do-Gon Ryu. 2007. Chemotherapy through mitochondrial apoptosis using nutritional supplements and herbs: A brief overview. *Journal of Bioenergetics and Biomembranes* **39**:1, 31-34. [CrossRef]
13. Stefan I. Liochev, Irwin Fridovich. 2007. The effects of superoxide dismutase on H2O2 formation. *Free Radical Biology and Medicine* **42**:10, 1465-1469. [CrossRef]
14. Jae Youl Cho. 2007. Immunomodulatory effect of nonsteroidal anti-inflammatory drugs (NSAIDs) at the clinically available doses. *Archives of Pharmacal Research* **30**:1, 64-74. [CrossRef]